Photoemission and x-ray absorption study of the electronic structure of $SrRu_{1-x}Ti_xO_3$

Jungho Kim,[1] J.-Y. Kim,[2] B.-G. Park,[3] and S.-J. Oh[1,*]
[1]*School of Physics Center for Strongly Correlated Materials Research, Seoul National University, Seoul 151-747, Korea*
[2]*Pohang Accelerator Laboratory, Pohang University of Science and Technology, Pohang, Korea*
[3]*Department of Physics and Electron Spin Science Center, Pohang University of Science and Technology, Pohang, Korea*
(Received 31 March 2006; revised manuscript received 24 May 2006; published 14 June 2006)

We investigated the chemical states and the electronic structure of $SrRu_{1-x}Ti_xO_3$ at room temperature by using both photoemission spectroscopy (PES) and x-ray absorption spectroscopy (XAS). The core-level spectra showed the absence of a macroscopic chemical inhomogeneity. The Ti $2p$ core level and the Ti $2p$ XAS reveal that the valency of Ti remains unchanged at 4+. In contrast to a previous PES study that was conducted on the scraped surfaces of polycrystal samples, we observed a systematic change in the Ru $4d$ band: a decrease in coherent peaks and an increase in incoherent peaks with an increase in x. In addition to this spectral change, we observed the depletion of the density of states near E_F. This depletion expands in energy and strength with an increase in x. Finally, the Ru $4d$ spectra for $x=0.8$ exhibit a hard gap. All these spectral changes are consistent with those reported in a recent optical and transport study.

DOI: 10.1103/PhysRevB.73.235109 PACS number(s): 79.60.Bm, 78.70.Dm, 71.30.+h

I. INTRODUCTION

Metal-insulator transition (MIT) is an intriguing phenomenon in transition metal oxides. At first consideration, an insulating ground state appears unlikely; however, this condition can be realized by electron correlations for integer filling in the framework of a Mott-Hubbard model. On the other hand, the disorder can induce an MIT in any filling case. With regard to the metallic case, Altshuler and Aronov predicted a disorder-induced $|E-E_F|^{1/2}$ dependence of the density of states (DOS) near E_F [in three dimensions (3D)].[1] With regard to the insulator, the localized carriers due to the Anderson localization show variable-range hopping (VRH) conductions despite the existence of a finite DOS at E_F: Mott VRH and Efros-Shklovskii (E-S) VRH.[2]

In a true system with strong correlations, when a disorder is introduced, two interactions, namely, the electron correlation and the disorder, are expected to compete with each other and change an initially metallic compound into an insulating one in a very interesting manner. A spectroscopic study on $LaNi_{1-x}M_xO_3$ (M=Mn and Fe) claimed to observe a disorder-induced $|E-E_F|^{1/2}$ cusp and an additive character of the electronic structures of intermediate compositions.[3] A theoretical study on the Hubbard model with a diagonal disorder in combination with the coherent potential approximation (CPA) showed that a strong disorder destroys low energy Fermi-Liquid coherence; moreover, in the case of a sufficiently large disorder, there is a continuous transition to a disordered insulating phase.[4]

$SrRu_{1-x}Ti_xO_3$ is a good candidate for the systematic investigation of the combined effects of disorder and correlation on the Ru $4d$ states because the structure is similar with each other and the Ti bands are adequately separated from the Ru bands. Recently, an optical and transport study was performed on $SrRu_{1-x}Ti_xO_3$ films grown by pulsed laser deposition (PLD).[5] In this study, intriguing electronic states were found between a correlated metal ($x=0.0$) and a band insulator ($x=1.0$). For $x\sim0.3$, the coherent band at E_F of a correlated metal ($x=0.0$) disappears due to the combined effects of disorder and correlation. Additionally, with a further increase in x, these combined effects change the metallic state to an insulating state such as that observed in an Anderson insulator ($x\sim0.5$) and a soft Coulomb gap insulator ($x\sim0.6$). For $x\sim0.8$, an optical gap of approximately 0.4 eV was observed.

The optical study on $SrRu_{1-x}Ti_xO_3$ reported a very broad Drude-like peak, which does not represent the quasiparticle (QP) peak; this peak was interpreted to be a signature of the disorder effect.[5] However, no disorder-induced changes in the Drude peak were observed directly because the optical spectra below 0.2 eV could not be obtained as a result of the strong multiphonon absorption of the $SrTiO_3$ substrate. Further, a spectroscopic study on $LaNi_{1-x}M_xO_3$ (M=Mn and Fe) was performed only for the metallic composition and not for the entire composition.[3] Hence, a spectroscopic study on the entire composition of the disordered Mott-Hubbard system is necessary to understand the combined effects of the electron correlation and the disorder.

Photoemission (PES) and x-ray absorption spectroscopy (XAS) are the most powerful tools for studying the chemical states of each element and the electronic structure of a solid. Previously, a PES and XAS study was conducted on the scraped surfaces of polycrystal $SrRu_{1-x}Ti_xO_3$ samples.[6] In contrast to the optical study, the authors of this study did not observe any changes in the shape of the Ru $4d$ spectra near E_F; thus, they concluded that the MIT of $SrRu_{1-x}Ti_xO_3$ is a simple percolation transition similar to that of metals embedded in a rare gas matrix. However, as pointed out in our PES study on $SrRuO_3$ prepared *in situ*,[7] the PES results for the scraped surfaces of polycrystal samples cannot be interpreted solely in terms of the electronic structure in the bulk due to the presence of many surface and grain boundary defect states.

In the present study, we present PES as well as XAS spectra of $SrRu_{1-x}Ti_xO_3$ films grown by PLD. In particular, the valence and core-level PES spectra were obtained using the clean film surface prepared *in situ*, without any additional surface cleaning processes. In our recent photoemission

study on an $SrRuO_3$ film, the use of a film surface prepared by *in situ* PLD proved to be effective for obtaining PES spectra representing the bulk property.[7] In fact, as shown below, we obtained spectra consistent with a recent optical and transport study on this system; this was in contrast to the previous PES study. For example, the valence band spectrum for $x=0.8$ exhibited a real gap, which was not observed in the previous PES study.

II. EXPERIMENTS

All the $SrRu_{1-x}Ti_xO_3$ targets were prepared using the solid state reaction method. The resulting powders were pressed into disk-shaped pellets and sintered in air at 1200 °C. The sintering procedure was repeated three times. All the $SrRu_{1-x}Ti_xO_3$ PLD films were prepared according to the procedure described in Ref. 7. It has been known that the $SrRu_{1-x}Ti_xO_3$ PLD films are grown epitaxially.[8–10] The high resolution x-ray diffraction (HRXRD) showed that our $SrRu_{1-x}Ti_xO_3$ films are *c*-axis oriented and epitaxial. And we have also confirmed the epitaxial growth of our $SrRu_{1-x}Ti_xO_3$ films by observing bright and streaky patterns in reflection high-energy electron diffraction (RHEED). The ultraviolet photoemission spectroscopy (UPS) experiments were performed using He *I* ($h\nu=21.2$ eV) in a chamber. This chamber was directly connected to the PLD growth chamber in order to enable the film prepared by PLD to be studied without additional cleaning processes. The Mg K_α line ($h\nu=1253.6$ eV) was used for the x-ray photoemission spectroscopy (XPS) measurements. The resolutions for UPS and XPS were 0.04 and 1.0 eV, respectively. The base pressure of our system was 1×10^{-10} Torr. The *ex situ* O 1*s* and Ti 2*p* absorption spectra were obtained in a total yield mode at the 2A beamline at Pohang Light Source (PLS) in Korea. The film samples grown by PLD at Seoul National University were taken out of the growth chamber and transported in air to Pohang Light Source. Before putting it into the XAS measurement chamber in PLS, the film surfaces were cleaned using acetone. Since the XAS technique is rather bulk sensitive, this treatment was enough to obtain clean spectra. The resolution was approximately 150 meV, and the base pressure during the XAS measurement was 1×10^{-10} Torr.

III. RESULTS AND DISCUSSION

A. Doping dependence of the chemical states: Core-level spectra

Figure 1 presents the core-level spectra of all the constituents (O, Sr, Ru, and Ti).[11] In Fig. 1(a), the Ru 3*d* and Sr 3*p* core levels are shown. The Ru 3*d* spectra exhibit a characteristic two-peak structure: screened peak and unscreened peak. The relative intensity of these two peaks is known to depend on the detailed valence feature of the Mott-Hubbard system.[12] In fact, the Ru 3*d* spectra exhibit a doping dependence change. We will discuss the spectral change of the Ru 3*d* core level with the evolution of the Ru 4*d* valence band in the later section. On the other hand, the Sr 3*p* spectra for all the compositions are those of single components. This is also the case for O 1*s* and Sr 3*d*, as shown in Figs. 1(b) and 1(c). The $SrRu_{1-x}Ti_xO_3$ materials used in the present experiment have different bonding combinations such as Ru-O-Ru, Ru-O-Ti, and Ti-O-Ti. Therefore, we can imagine that the end members may show different core-level positions due to the initial state effects such as the Madelung potential: therefore, the core-level spectra of the intermediate compositions may show a multipeak structure due to the chemical inhomogeneity. The fact that all the core-level spectra show single peak structures implies that there are no chemical inhomogeneities and that all the bonding combinations are thoroughly mixed in the atomic scale. Actually, the effective-medium approximation (EMA) analysis of the optical spectra eliminated the possibility of chemical inhomogeneity.[5]

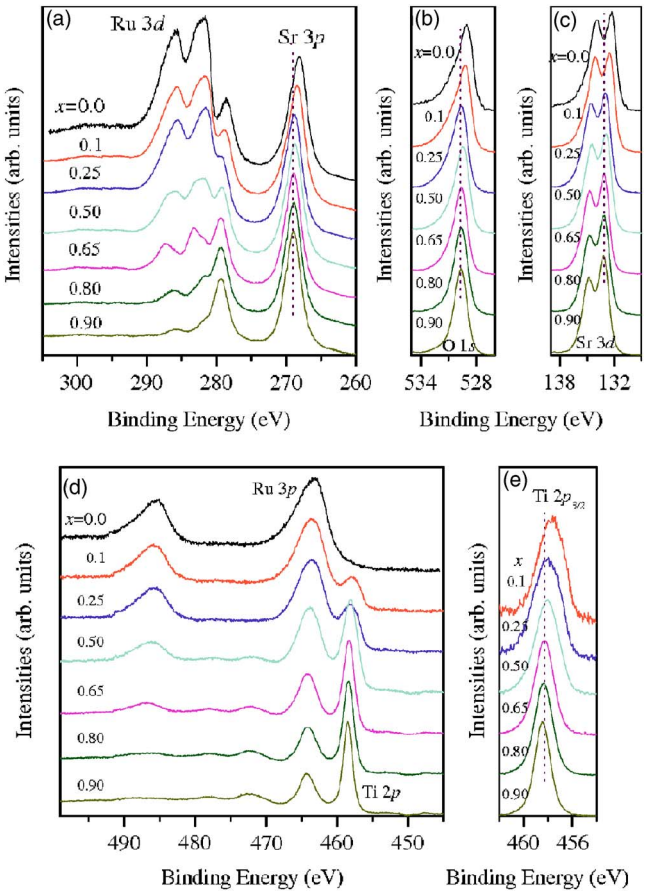

FIG. 1. (Color online) Core-level spectra for $SrRu_{1-x}Ti_xO_3$ ($x=0.0$, 0.1, 0.25, 0.50, 0.65, 0.8, and 0.9). (a) Ru 3*d* and Sr 3*p*. (b) O 1*s*. (c) Sr 3*d*. (d) 3*p* and Ti 2*p*. (e) Ti $2p_{2/3}$ core-level spectra that are obtained by subtracting the overlapped high binding energy contributions.

The other obvious changes are the core-level shifts and the asymmetric line shapes. The O 1*s*, Sr 3*d*, and 3*p* core levels shift toward higher binding energies with an increase in *x*, as shown in Figs. 1(a)–1(c). These core-level shifts will be discussed in the later section in detail. For $x<0.8$, which has a finite DOS at E_F,[5] these core-level spectra exhibit asymmetric line shapes, which indicates the effects of metallic screening on the spectra. The extent of this asymmetry decreases with an increase in *x*.

The large energy separation between Ti $3d$ and Ru $4d$ (1.8 eV) is thought to decouple these two bands, thereby preventing charge fluctuations between the Ru $4d$ states at E_F and the Ti $3d$ states.[5,6] The authors of the optical study arrived at this conclusion through the spectral weight analyses of optical conductivity over an interband transition region.[5] Further, the authors of the previous PES and XAS study expressed a similar view on this issue.[6] Figure 1(e) exhibits the Ti $2p_{3/2}$ core-level spectra that are obtained by subtracting the overlapping high binding energy contributions. No signature of Ti^{3+} could be identified since the so-called "chemical shift" due to a decrease in the Ti valence from Ti^{4+} toward Ti^{3+} is reported to be approximately 1.5 eV.[13] On the other hand, the $2p_{3/2}$ core level peaks are broadened with a decrease in x. This core-level broadening suggests the occurrence of some small changes in the chemical environments around the Ti sites because the core-level PES probes the local chemical states at specific lattice sites. At present, the origin of the broadening is unclear. The broadened spectrum for $x=0.1$ is found to be fitted by an increase in Gaussian broadening with a Lorentzian broadening similar to that of the core-level spectrum for $x=0.9$, while an increase in the Lorentzian broadening yields an unsatisfactory result. Therefore, similar to the case of a disordered binary alloy such as $Cu_{1-x}Pd_x$, the disordered broadenings of core-level spectra of a Gaussian nature can exist.[14]

B. Doping dependence of the chemical states: X-ray absorption spectra

Figure 2 presents the Ti $2p$ XAS spectra for the entire compositions that were measured at PLS. These Ti $2p$ XAS spectra are obtained by subtracting the Ru $3p$-$4d$ XAS contributions, which have similar energies. Since the Ru $3p$-$4d$ XAS spectrum does not have a complex structure, the overall spectral shape is hardly affected. In particular, the spectra below 465 eV can be interpreted in terms of only Ti $2p$ XAS because the Ru $3p$-$4d$ XAS spectra are devoid of intensity below 465 eV, as shown in Fig. 2(a). The Ti $2p$ XAS spectra for $SrTiO_3$ presented in Fig. 2(a) are consistent with the published data.[15,16] The four intense peaks distributed from 462 to 472 eV can be assigned as $2p_{3/2}t_{2g}$(A), $2p_{3/2}e_g$(B), $2p_{1/2}t_{2g}$, and $2p_{1/2}e_g$ based on the calculation of the dipole transition probability from Ti $3d^0$ to $2p^53d^1$. In the octahedral symmetry, the $2p_{3/2}$ and the $2p_{1/2}$ manifolds have five and two levels, respectively. The two small pre-edge structures originate from the remaining three levels. Based on the well-resolved two pre-edge structures shown in the inset of Fig. 2(b), we can confirm that the experimental resolution ($\sim$150 meV) is very good. However, the origin of the satellite structures above 472 eV—whether the charge-transfer-type satellite or the polaronic satellite—remains controversial.[16,17]

The four major peaks of the $2p$ XAS spectra exhibit some changes with a decrease in the Ti concentration. To enable a closer examination of the changes, the expanded spectra below 468 eV are presented in Fig. 2(b). The position of peak A shifts toward the lower photon energy by 0.1 eV, while the photon energy of peak B decreases by 0.25 eV. As a result,

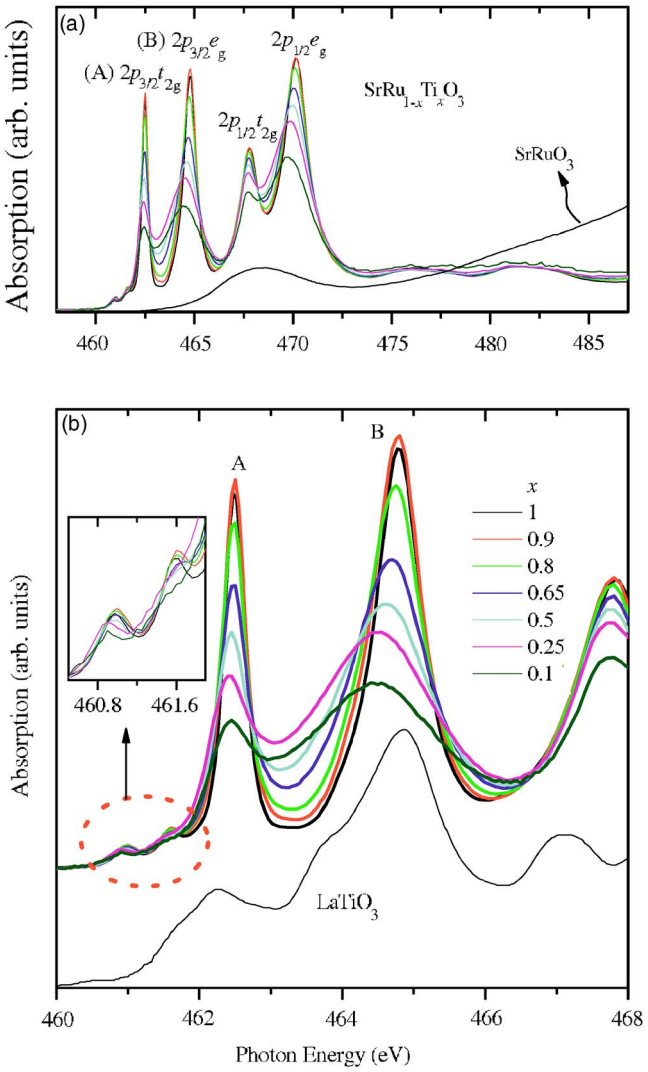

FIG. 2. (Color online) Ti $2p$ x-ray absorption (XAS) spectra for $SrRu_{1-x}Ti_xO_3$. ($x=0.0$, 0.1, 0.25, 0.50, 0.65, 0.8, 0.9, and 1.0) are shown in (a). The expanded view of Ti L_3 XAS is exhibited in (b). The spectrum of $LaTiO_3$ from Ref. 19 is presented for comparison. The pre-edge peaks are expanded in the inset of (b).

the energy difference between peaks A and B becomes 0.15 eV; this difference is smaller in the case of $x=0.1$ than in $x=1$. The energy separation of A and B is a measure of the crystal field splitting, 10 Dq. The crystal field splitting is a strong function of the distance between transition metal and oxygen. The Ru-O distance of $SrRuO_3$(1.985 Å) is larger than the Ti-O distance of $SrTiO_3$(1.95 Å).[18] Therefore, in the case of $x=0.1$, the Ti-O distance is larger than that for $x=1.0$, and the decrease in the energy separation of A and B is reasonable.

The more appreciable change that occurs with a decrease in x is the broadening of all the structures. Compared with the d^0 systems such as $SrTiO_3$, the d^1 systems such as $LaTiO_3$ have more multiplet states, and thus, the feature is broader.[19] Figure 2(b) presents the Ti $2p$ XAS spectrum of $LaTiO_3$ from Ref. 19. $LaTiO_3$ is a representative system for Ti^{3+} in the octahedral symmetry (orthorhombic structure). The feature is complex and broader despite the resolution

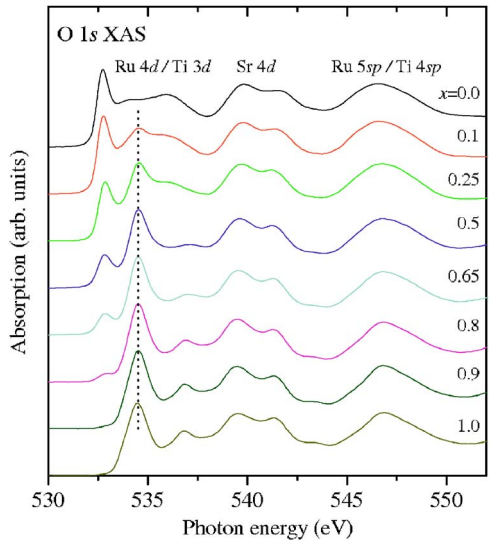

FIG. 3. (Color online) O 1*s* x-ray absorption (XAS) spectra for $SrRu_{1-x}Ti_xO_3$. (x=0.0, 0.1, 0.25, 0.50, 0.65, 0.8, 0.9, and 1.0).

(150 meV) being similar to that presented in our data. However, the x=0.1 spectrum does not resemble the spectrum of $LaTiO_3$. Firstly, the energy separation of the two major peaks is different. Secondly, as shown in the inset of Fig. 2(b), the spectrum of x=0.1 still exhibits the two pre-edge structures, which are absent in the case of $LaTiO_3$. Therefore, it can be concluded that $SrRu_{1-x}Ti_xO_3$ has no Ti^{3+} component. As discussed in the previous section, the core-level spectrum of Ti 2*p* becomes broader with a decrease in x. Hence, the broadened feature of the Ti 2*p* XAS spectrum for small x may be due to the broadening of the 2*p* core level.

Figure 3 presents the O 1*s* XAS spectra for the entire compositions. The end member spectra ($SrRuO_3$ and $SrTiO_3$) are consistent with the previously published data.[20–22] In the case of $SrRuO_3$, the absorptions below 538 eV, which have three distinct peaks, are related to the O 2*p* states hybridized with Ru 4*d*. The first peak is mostly related with t_{2g}, while the third is related with e_g. Both the upper Hubbard bands (UHB) of t_{2g} and e_g contribute to the spectral weight of the second small peak. The absorptions above these structures result due to the hybridization with the Sr 4*d* states. The emissions at the highest energies originate from Ru 5*sp* and Ti 4*sp*. The first peak for $SrTiO_3$ is related to t_{2g}. The e_g band extends from 537 to 540 eV. The second small peak, which cannot be predicted from the band structure calculation, is known to exist due to the effect of the core-hole potential.[23]

The absorptions above 538 eV (Sr 4*d*, Ru 5*sp*, and Ti 4*sp*) do not exhibit any obvious feature change with x. On the other hand, the absorptions below 538 eV (Ru 4*d* and Ti 3*d*) exhibit systematic spectral changes: the 533 eV peak, which is related to the Ru t_{2g} states, loses its spectral weight, and the second peak around 534.5 eV, which is related to the Ti t_{2g} states, gains its spectral weight. Based on the end member spectra, the energy difference of the t_{2g} states of Ti and Ru was estimated to be 1.8 eV. This difference hardly changes with x. $SrTiO_3$ is a band insulator, and there are many accessible Ru 4*d* states below the Ti t_{2g} states. Therefore, in principle, it is energetically unfavorable that the Ti t_{2g} states are filled, and Ti has a 3+ valency at the expense of energy of 1.8 eV. This is consistent with our observation of the absence of Ti^{3+} in the Ti 2*p* XPS spectra and Ti 2*p* XAS spectra.

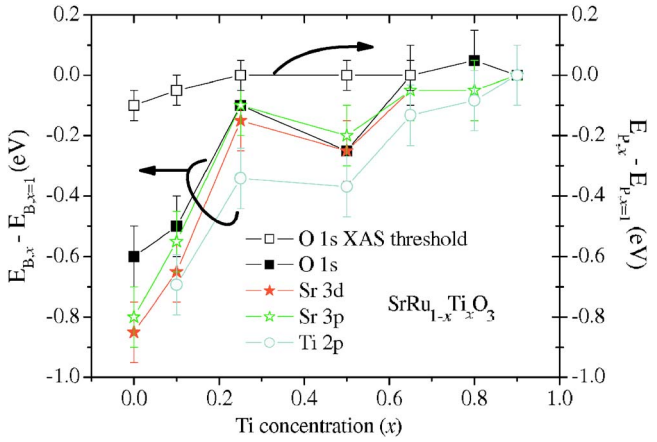

FIG. 4. (Color online) Shifts in the O 1*s*, Sr 3*d*, Sr 3*p*, and Ti 2*p* core levels are summarized. The shift in the O 1*s* XAS threshold is included.

C. Doping dependence of the chemical states: Core-level shifts

Figure 4 summarizes the core-level shifts of all the constituents, except Ru; these shifts are measured relative to x =1. In the case of the Ru peaks, it is impossible to determine the core-level shifts unambiguously because of the multipeak structures due to the different screening channels.[12] The peak positions of O 1*s*, Sr 3*d*, Sr 3*p*, and Ti 2*p* are shifted toward higher binding energies with an increase in x. There are roughly two different regions as a function of doping. The shifts occur rapidly below x=0.3. On the other hand, the core levels shift gradually above x=0.3.

The experimental XPS binding energy shift ΔE of the core level measured relative to the Fermi level is given by $\Delta E_B = \Delta E_F - K\Delta Q + \Delta V_M - \Delta E_R$, where the first term is the change in the Fermi energy, the second term is the so-called "chemical shift," the third term is the change in the Madelung potential, and the last term is the change in the extra-atomic relaxation energy of the core-hole state.[24] In our case, the XPS and XAS analyses revealed no valency changes. Hence, the chemical shift may not be a dominant parameter. The origin of the shifts cannot be ΔV_M because the core levels of the anion (O) and cations (Sr and Ti) show similar core-level shifts. Therefore, the possible sources of these core-level shifts are ΔE_F and ΔE_R. The O 1*s* XAS threshold also reflects the chemical potential shift.[25,26] In our case, as compiled in Fig. 4, the O 1*s* XAS threshold shift occurs only below x=0.3, and the total shift is only 0.1 eV. Thus, the chemical potential shift does not account for the core-level shifts. As mentioned above, a metallic screening is evident from the asymmetric line shapes of the core levels (O 1*s*, Sr 3*d*, Sr 3*p*, and Ti 2*p*). Therefore, at present, it is reasonable to attribute the remaining core-level shifts to ΔE_R.

D. Metal-insulator transition: Valence band spectra

The Ru 3*d* core-level spectra for x=0, 0.1, 0.25, 0.5, and 0.65 are displayed in Fig. 5. These spectra were obtained by

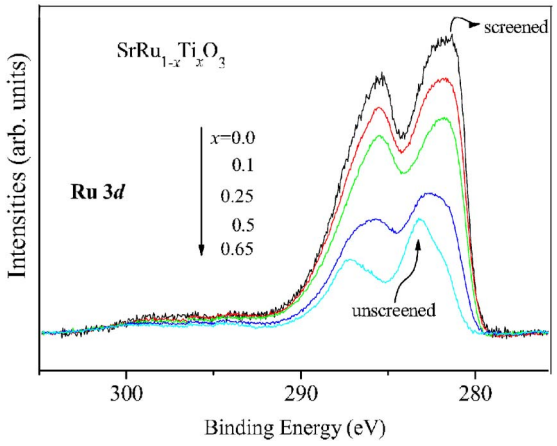

FIG. 5. (Color online) Ru 3*d* core-level spectra for $x=0.0$, 0.1, 0.25, 0.5, and 0.65. The overlapping signal from Sr 3*p* and the Shirley-type background are subtracted.

subtracting the Sr $3p_{1/2}$ and $3p_{3/2}$ emissions from the data shown in Fig. 1(a). Additionally, the background emission is subtracted based on the Shirley method. In our spectra, the *C* 1*s* peak that overlaps with Ru $3d_{1/2}$ is minimal, and the spectral weight of the screened peak in our Ru 3*d* spectrum for $SrRuO_3$ is considerably larger than that reported in previously published data, which were obtained using a polycrystal.[27] Based on the recent dynamical mean-field theory, it was reported that the multipeak structure of the Ru 3*d* core level is due to the different screening mechanisms of the Mott-Hubbard model.[12] The lower binding energy structure (screened) is due to the coherent band or the quasiparticle metallic screening, while the higher binding energy structure (unscreened) originates from the incoherent band or lower Hubbard band (LHB) screening. Thus, the Ru 3*d* core-level spectra reflect the MIT of the Mott-Hubbard system. When $x=0$ is compared with $x=0.1$, a slight suppression of the screened peak is observed. On the other hand, the screened peak shows an obvious decrease for $x=0.5$ indicating the MIT. Since the core-hole screening occurs locally, an important criterion for the screened peak is the existence of a finite DOS at E_F. In fact, the screened peak of the Ru 3*d* core level exists in the Ru 3*d* spectrum of $Y_{1.6}Bi_{0.4}Ru_2O_7$, which shows a VRH-type conduction.[28] The Ru 3*d* core-level spectrum of the $x=0.5$ sample, which exhibits VRH-type conduction, is very similar to that of $Y_{1.6}Bi_{0.4}Ru_2O_7$. Moreover, the suppression of the screened peak becomes evident for $x=0.65$.

Figure 6(a) presents the He I spectra of the valence bands for all the compositions. As reported in Ref. 7, the spectrum for $x=0$ exhibits well-resolved structures. The emissions above 2.5 eV are from the O 2*p* bonding and nonbonding states, while the signals below 2.5 eV are from the Ru 4*d* antibonding states.[7] Similar to the $x=0.0$ spectrum, all the other spectra show well-resolved structures. According to Higuchi *et al.*, the calculated O 2*p* band of $SrTiO_3$ has two peak structures.[29] Their experimental data show a considerably broadened peak structure. On the other hand, our data for $x=0.9$ clearly show two peak structures.

To demonstrate the manner in which the Ru 4*d* feature changes with *x*, in Fig. 6(b), we present the Ru 4*d* feature

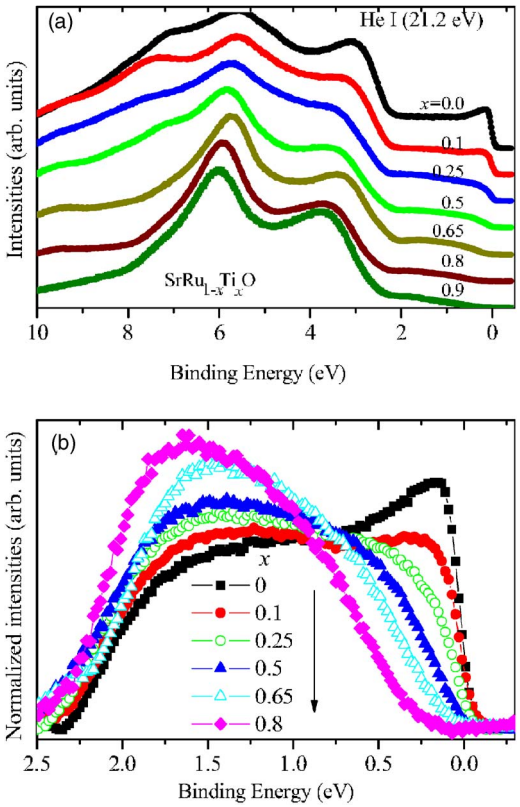

FIG. 6. (Color online) UPS spectra obtained with He *I* ($h\nu=21.2$ eV). In (a), all valence band spectra are presented. (b) Changes in the Ru 4*d* feature are shown. These spectra are obtained by subtracting the O 2*p* contributions from the raw data; these contributions are assumed to have a Gaussian shape and are normalized to yield the same area.

that was prepared by subtracting the O 2*p* contributions from the high binding energy structures, which are assumed to have a Gaussian shape. For the purpose of comparison, all the spectra are normalized to yield the same integrated spectral weight. The change in the Ru 4*d* feature, which was not observed in the previous PES study on the scraped surface of the polycrystal sample, is consistent with the spectral change reported in the recent optical and transport study of $SrRu_{1-x}Ti_xO_3$ (Ref. 5). At a small doping level ($0.2<x\leq 0$), $SrRu_{1-x}Ti_xO_3$ can be categorized as a correlated metal. The coherent peaks are clearly observed for $x=0$ and 0.1. At $x=0.3$, the coherent peak was reported to be absent in the optical data.[5] Correspondingly, our spectrum for $x=0.25$ does not exhibit a coherent peak. With further doping, $SrRu_{1-x}Ti_xO_3$ was found to become a disordered correlation insulator similar to an Anderson insulator and a soft Coulomb gap insulator. In our spectra, the density of state (DOS) at E_F remains finite until $x=0.65$ and finally the hard gap opens at $x=0.8$. On the other hand, in the previous PES study on polycrystal samples, this gap was not observed even in the case of $x=0.9$ (Ref. 6). The difference in the two PES studies is possibly due to the dissimilar type of samples (film and polycrystal) and the different preparation methods of the surface. In the optical study, an optical gap of 0.4 eV was reported for the same composition. In our case, the upturn

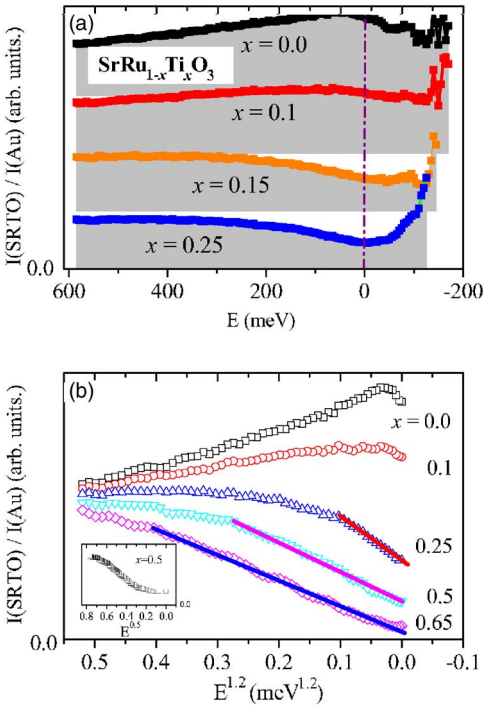

FIG. 7. (Color online) (a) The spectra for $x=0.0$, 0.1, 0.15, and 0.25 divided by the room temperature Au reference spectrum are presented. The depletion of DOS near E_F develops with an increase in x. In (b), the spectra of (a) are plotted as a function of $E^{1.2}$ to demonstrate the energy dependence of the depletion of the DOS. Inset: The spectrum for $x=0.5$ is plotted as a function of $E^{0.5}$ for the purpose of comparison.

point is approximately 0.2 eV. Assuming a symmetric gap opening, the total gap size can be estimated to be 0.4 eV. Thus, our spectrum for $x=0.8$ is consistent with the optical spectrum reported in the recent study.[5] With a decrease in the DOS near E_F, the incoherent peak shifts slightly toward higher energy.

E. Metal-insulator transition: Depletion of DOS

Figure 7(a) shows the spectra for $x=0.0$, 0.1, 0.15, and 0.25 divided by the room temperature Au reference spectrum. In the framework of the Mott-Hubbard model, the MIT of $SrRu_{1-x}Ti_xO_3$ is induced by bandwidth narrowing because it is assumed that the electron correlation (U) would not change to a considerable extent with x. However, even the spectrum for $x=0.1$, which still exhibits a coherent peak, does not show the narrowing of the Ru t_{2g} band. Compared with $SrRuO_3$, only the spectral weight of the coherent peak near E_F is reduced. Thus, bandwidth narrowing does not appear to be the factor responsible for the spectral evolution of $SrRu_{1-x}Ti_xO_3$.

On the other hand, in the spectra for $x=0.15$ and 0.25, the depletion of the DOS is observed to develop. In the case of the metallic compositions of $LaNi_{1-x}M_xO_3$ (M=Mn and Fe), the $E^{0.5}$-dependent DOS depletion was reported to be observed.[3] However, in our spectra for $x=0.15$ and 0.25, the depleted DOS does not show this $E^{1/2}$ singularity. To demonstrate the energy dependence of the depletion, the spectra of Fig. 7(a) are rescaled on the energy axis in Fig. 7(b). It is found that the DOS of $x=0.25$, 0.5, and 0.65 exhibit an $E^{1.2}$ dependence. For the purpose of comparison, we have plotted the spectrum for $x=0.5$ as a function of $E^{0.5}$ in the inset. With an increase in x, the depletion region expands in energy and strength, and the DOS at E_F attains a zero value at $x\sim0.7$, which defines the critical point of MIT. Further, the hard gap of 0.4 eV opens at $x=0.8$.

This $E^{1.2}$ dependence of the DOS is different from the soft Coulomb gap characterized by E^2 dependence; this gap opens up due to the electron-electron Coulomb repulsion.[2] The linear energy dependence of DOS has been observed in the cuprates and manganites that are near MIT instability.[30,31] A recent high resolution PES study on $BaIrO_3$, which exhibits concurrent ferromagnetism with a charge density wave transition, reported an $E^{1.5}$ dependence of the DOS near E_F.[32] The electron-phonon or electron-magnon couplings are considered to influence the electronic structure of these strongly correlated systems and modify the DOS in this unusual fashion. In the case of a disordered system, a similar phenomenon has been reported. In $LaNi_{0.8}Mn_{0.2}O_3$, which is semimetallic, the conductance was reported to be linear at an applied voltage V.[3] The depletion of DOS has also been reported to occur in disordered alloys such as Cu-Pt and Cu-Ni.[33] In this case, the energy dependence of the depleted DOS does not exhibit a $|E-E_F|^{1/2}$ singularity near E_F, but an almost linear dependence.

The one-band Hubbard model with a static diagonal disorder has been the subject of several studies.[4,34–37] The studies evaluating the effects of disorder by a simple weighting procedure[34–37] similar to the virtual crystal approximation (VCA) for alloys[38] predicted that the electronic structure of a substituted system can be obtained following an additive average of the electronic structure of the end members. The experimental bremsstrahlung isochromat spectra (BIS) of $LaNi_{1-x}Mn_xO_3$ were reported to follow this prediction.[3] However, within these theoretical frameworks, the unusual modification of the DOS near the E_F of $SrRu_{1-x}Ti_xO_3$ cannot be explained.

On the other hand, a theoretical study of the Hubbard model with a diagonal disorder in combination with CPA suggested that the low energy Fermi-liquid coherence is destroyed by strong disorder and the gap opens with an increase in disorder.[4] Qualitatively, this theoretical result is in accordance with our experimental result. In $SrRu_{1-x}Ti_xO_3$, a disorder to the extent of 1.8 eV, which is comparable to the onsite Coulomb repulsion energy U, is strong enough to destroy the low energy Fermi-liquid coherence. Moreover, the origin of the gap in the case of $x=0.8$ can be properly understood in this context. However, at present, it is unclear whether the effects of electron correlation and strong disorder can quantitatively lead to the unusual $E^{1.2}$ dependence of DOS.

F. Metal-insulator transition: Percolation

As noted in the recent optical and transport study, our study reveals that the combined effects of the disorder

and correlation play an important role in the MIT of $SrRu_{1-x}Ti_xO_3$. However, the previous PES study on the polycrystal samples concluded that the electron correlation effects do not play a major role and the MIT is a percolation transition.[6] These conclusions are primarily based on two conditions: (i) there are no charge fluctuations from the Ru 4*d* states at E_F to the Ti 3*d* states due to the large energy separation of the Ti 3*d* and the Ru 4*d* bands and (ii) the overall shape, bandwidth, and peak position of the Ru 4*d* band do not vary with x. The first point is consistent with our observations of the absence of Ti^{3+} in the XPS and XAS spectra. The second point, that is, the absence of changes in the shape of the Ru 4*d* band may imply that there is a macroscopic chemical segregation/inhomogeneity. However, our core-level spectra suggest that a macroscopic chemical segregation is unlikely. In addition, we observed a systematic change in the Ru 4*d* states. In particular, a hard gap opens in the case of $x=0.8$. Therefore, as noted in the recent optical and transport study, the simple percolative MIT, which was suggested in the previous PES study, does not apply in this system.

However, the percolation phenomenon may still play some role in this system. We noted that the electrons from the Ru 4*d* states cannot reside in the Ti sites because there are no accessible states even when both Ru and Ti are microscopically distributed in a random manner. Therefore, the existence of the percolation path is a necessary condition for the electrons to contribute to the conduction. Thus, in addition to the electron correlations and the disorder potential, it is essential to consider percolation as one of the factors driving the MIT. Interestingly, the critical doping (x_c) for MIT is 0.3 for both the polycrystal samples and the film samples.[5,6] This may not be a casual coincidence. Further, based on the recent *in situ* thickness-dependent PES study on $SrRuO_3$ films deposited on $SrTiO_3$ substrates, it is evident that at the initial stage, the films show three-dimensional (3D) islands and the Ru 4*d* spectra of these films exhibit an energy gap at E_F.[39] A finite DOS at E_F begins to appear when a coalescence of 3D islands comes into existence. Therefore, the chemical/electronic phase separation at the nanoscale level and the related percolation of $SrRu_{1-x}Ti_xO_3$ need to be investigated. In this respect, it would be interesting to examine the real-space images of the local electronic properties of $SrRu_{1-x}Ti_xO_3$ obtained by scanning tunneling spectroscopy.

IV. SUMMARY

We present simultaneous analyses of UPS, XPS, and XAS measurements of $SrRu_{1-x}Ti_xO_3$ films grown by PLD. In contrast to the scraped surface of polycrystal samples used in the previous PES study, we observed that our film surface, which was prepared *in situ*, did not exhibit macroscopic chemical inhomogeneity based on an examination of the core-level spectra. As expected from the large energy difference between the Ti t_{2g} and the Ru t_{2g} states, the Ti 2*p* core level and the Ti 2*p* x-ray absorption spectra reveal that the 4+ valency of Ti remains unchanged. With an increase in x, the ratio of the coherent-to-incoherent spectral weights of the Ru 4*d* states is found to decrease. In addition, we observed that the DOS depletion near E_F expand in energy and strength with an increase in x and finally drives $SrRu_{1-x}Ti_xO_3$ to an insulating state. This DOS depletion and the related MIT can be properly understood in terms of the combined effects of electron correlations and disorder potentials. The issue of percolation requires clarification by further investigations such as the examination of the real-space images of the local electronic properties of $SrRu_{1-x}Ti_xO_3$ obtained by scanning tunneling spectroscopy.

ACKNOWLEDGMENTS

We would like to thank K. W. Kim for useful discussions. This work was supported by the KOSEF through CSCMR.

*Corresponding author. Electronic address: sjoh@phya.snu.ac.kr

[1] B. L. Althsuler and A. G. Aronov, Solid State Commun. **30**, 115 (1979).
[2] A. L. Efros and B. I. Shklovskii, J. Phys. C **8**, L49 (1975).
[3] D. D. Sarma, A. Chainani, S. R. Krishnakumar, E. Vescovo, C. Carbone, W. Eberhardt, O. Rader, C. Jung, C. Hellwig, W. Gudat *et al.*, Phys. Rev. Lett. **80**, 4004 (1998).
[4] M. S. Laad, L. Craco, and E. Muller-Hartmann, Phys. Rev. B **64**, 195114 (2001).
[5] K. W. Kim, J. S. Lee, T. W. Noh, S. R. Lee, and K. Char, Phys. Rev. B **71**, 125104 (2005).
[6] M. Abbate, J. A. Guevara, S. L. Cuffini, Y. P. Mascarenhas, and E. Morikawa, Eur. Phys. J. B **25**, 203 (2002).
[7] J. Kim, J. Chung, and S.-J. Oh, Phys. Rev. B **71**, 121406(R) (2005).
[8] A. Gupta, B. W. Hussey, and T. M. Shaw, Mater. Res. Bull. **31**, 1463 (1996).
[9] R. Ohara, T. Schimizu, K. Sano, M. Yoshiki, and T. Kawakubo, Jpn. J. Appl. Phys., Part 1 **40**, 1384 (2001).
[10] L. Miéville, T. H. Geballe, L. Antognazzab, and K. Char, Appl. Phys. Lett. **70**, 126 (1997).
[11] The spectra for $SrTiO_3$ film could not be taken due to the severe charging effect. This is also the case for He *I* spectra.
[12] H.-D. Kim, H.-J. Noh, K. H. Kim, and S.-J. Oh, Phys. Rev. Lett. **93**, 126404 (2004).
[13] K. Morikawa, T. Mizokawa, A. Fujimori, Y. Taguchi, and Y. Tokura, Phys. Rev. B **54**, 8446 (1996).
[14] R. J. Cole, N. J. Brooks, and P. Weightman, Phys. Rev. Lett. **78**, 3777 (1997).
[15] M. Abbate, F. M. F. de Groot, J. C. Fuggle, A. Fujimori, Y. Tokura, Y. Fujishima, O. Strebel, M. Domke, G. Kaindl, J. van Elp *et al.*, Phys. Rev. B **44**, 5419 (1991).
[16] G. van der Laan, Phys. Rev. B **41**, 12366 (1990).
[17] Y. Harada, T. Kinugasa, R. Eguchi, M. Matsubara, A. Kotani, M. Watanabe, A. Yagishita, and S. Shin, Phys. Rev. B **61**, 12854 (2000).

[18] C. Eylem, H. L. Ju, B. W. Eichhorn, and R. L. Greene, Solid State Chem. **114**, 164 (1995).
[19] M. W. Haverkort, Z. Hu, A. Tanaka, G. Ghiringhelli, H. Roth, M. Cwik, T. Lorenz, C. Schüßler-Langeheine, S. V. Streltsov, A. S. Mylnikova *et al.*, Phys. Rev. Lett. **94**, 056401 (2005).
[20] J. Okamoto, T. Mizokawa, A. Fujimori, I. Hase, M. Nohara, H. Takagi, Y. Takeda, and M. Takano, Phys. Rev. B **60**, 2281 (1999).
[21] J. Park, S.-J. Oh, J.-H. Park, D. M. Kim, and C.-B. Eom, Phys. Rev. B **69**, 085108 (2004).
[22] A. Fujimori, I. Hase, M. Nakamura, H. Namatame, Y. Fujishima, Y. Tokura, M. Abbate, F. M. F. de Groot, M. T. Czyzyk, J. C. Fuggle *et al.*, Phys. Rev. B **46**, 9841 (1992).
[23] F. M. F. de Groot, J. Faber, J. J. M. Michiels, M. T. Czyzyk, M. Abbate, and J. C. Fuggle, Phys. Rev. B **48**, 2074 (1993).
[24] A. Ino, T. Mizokawa, A. Fujimori, K. Tamasaku, H. Eisaki, S. Uchida, T. Kimura, T. Sasagawa, and K. Kishio, Phys. Rev. Lett. **79**, 2101 (1997).
[25] K. Kobayashi, T. Mizokawa, A. Ino, J. Matsuno, A. Fujimori, H. Samata, A. Mishiro, Y. Nagata, and F. M. F. de Groot, Phys. Rev. B **59**, 15100 (1999).
[26] T. Saitoh, A. E. Bocquet, T. Mizokawa, H. Namatame, A. Fujimori, M. Abbate, Y. Takeda, and M. Takano, Phys. Rev. B **51**, 13942 (1995).
[27] P. Cox, R. Egdell, J. Goodenough, A. Hamnett, and C. Naish, J. Phys. C **16**, 6221 (1983).
[28] S. Yoshii and M. Sato, J. Phys. Soc. Jpn. **68**, 3034 (1999).
[29] T. Higuchi, T. Tsukamoto, N. Sata, M. Ishigame, Y. Tezuka, and S. Shin, Phys. Rev. B **57**, 6978 (1998).
[30] H. D. Hudspeth, F. Sharifi, I. J. Guilaran, P. Xiong, and S. von Molnar, Phys. Rev. B **65**, 052405 (2002).
[31] M. Fath, S. Freisem, A. A. Menovsky, Y. Tomioka, J. Aarts, and J. A. Mydosh, Science **285**, 1540 (1999).
[32] K. Maiti, R. S. Singh, V. R. R. Medicherla, S. Rayaprol, and E. V. Sampathkumaran, Phys. Rev. Lett. **95**, 016404 (2005).
[33] H.-J. Noh, T.-U. Nahm, J.-Y. Kim, W.-G. Park, S.-J. Oh, J.-P. Hong, and C.-O. Kim, Solid State Commun. **116**, 137 (2000).
[34] V. Janis and D. Vollhardt, Phys. Rev. B **46**, 15712 (1992).
[35] V. Dobrosavljevic and G. Kotliar, Phys. Rev. Lett. **71**, 3218 (1993).
[36] D. D. Sarma, S. R. Barman, H. Kajueter, and G. Kotliar, Europhys. Lett. **36**, 307 (1996).
[37] T. Mutou, Phys. Rev. B **60**, 2268 (1999).
[38] R. J. Elliott, J. A. Krumhansl, and P. L. Leath, Rev. Mod. Phys. **46**, 465 (1974).
[39] D. Toyota, I. Ohkubo, H. Kumigashira, M. Oshima, T. Ohnishi, M. Lippmaa, M. Takizawa, A. Fujimori, K. Ono, M. Kawasaki *et al.*, Appl. Phys. Lett. **87**, 162508 (2005).